Nano Energy 105 (2023) 108015

Contents lists available at ScienceDirect

Nano Energy

journal homepage: www.elsevier.com/locate/nanoen

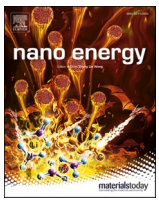

Transient energy trapping as a size-conserving surface passivation strategy for producing bright ultrasmall upconversion nanoprobes

Fuhua Huang [a,c], Lucía Labrador-Páez [b], Hans Ågren [a,c,*], Li Wang [a,c,*], Jinglai Zhang [a,c,*], Rui Pu [d], Qiuqiang Zhan [d,e], Jerker Widengren [b], Haichun Liu [b,**]

[a] College of Chemistry and Chemical Engineering, Henan University, Kaifeng, Henan 475004, PR China
[b] Department of Applied Physics, KTH Royal Institute of Technology, S-10691 Stockholm, Sweden
[c] Henan Center for Outstanding Overseas Scientists, Henan University, Kaifeng 475004, PR China
[d] Centre for Optical and Electromagnetic Research, Guangdong Provincial Key Laboratory of Optical Information Materials and Technology, South China Academy of Advanced Optoelectronics, South China Normal University, Guangzhou 510006, PR China
[e] MOE Key laboratory & Guangdong Provincial Key Laboratory of Laser Life Science, Guangdong Engineering Research Centre of Optoelectronic Intelligent Information Perception, South China Normal University, Guangzhou 510631, PR China

ARTICLE INFO

Keywords:
Upconversion nanoparticles
Ultrasmall nanoparticles
Energy trapping
Energy migration
Surface quenching
Cell imaging

ABSTRACT

Lanthanide-doped upconversion nanoparticles (UCNPs) have been widely exploited as nanoprobes or energy transducers in traditional as well as emerging biological applications, such as bioimaging, photodynamic therapy, optogenetics, gene editing. However, the breadth and depth of their utility in the biomedical areas are still not comparable to conventional luminescent probes, such as fluorescent dyes and semiconductor quantum dots. Their application is largely limited by their large size, typically > 20 nm, to ensure a sufficient luminescence brightness. In order to enhance the brightness of UCNPs without exceeding the critical size limitations for biomedical applications, we employ here a transient energy trapping effect as a nanoprobe surface passivation strategy to prevent deleterious distant energy migration in the host lattice, which is particularly prevalent in ultrasmall UCNPs and leads to luminescence quenching. We demonstrate this strategy by incorporating Tm^{3+} ions as energy trapping centers near the surface of sub-10 nm $NaYF_4$: Yb, Er UCNPs and obtain an emission enhancement by almost one order of magnitude without any increment on the nanoparticle size. Our work presents a promising strategy for the preparation of ultrasmall and bright upconversion nanoprobes that are less vulnerable to surface quenching and that potentially minimize the interference with the object. This facilitates their biomedical applications as here demonstrated by unprecedented high-quality cell labeling and imaging, featured with very uniform nanoparticle distribution in the outer nuclear region.

1. Introduction

Exogenous luminophores are widely used as probes in biological studies in the life sciences. In order to minimize the disturbance of these probes with the target to provide more accurate intrinsic information, it is often demanded that the size of the used probes is within the sub-10 nm range. Most extensively used luminescent probes include a variety of emitters like organic dyes [1,2], fluorescence proteins, and semiconductor quantum dots [3,4], which, however, often show shortcomings such as photobleaching, photoblinking, and spectral overlapping with the autofluorescence of biological tissues [5]. The use of alternative lanthanide-doped upconversion nanoparticles (UCNPs) in biomedical areas has attracted increasing attention, not only in traditional bioimaging applications [6–10], but also in emerging applications such as optogenetics [11,12] and gene editing [13]. These applications benefit from several remarkable advantages of UCNPs, such as high photostability, high chemical stability, low toxicity, large imaging depth, absence of autofluorescence interference, and minimum damage to the biological specimen [14].

Although the unique optical properties of UCNPs are attractive for numerous biomedical applications [15,16], they still remain disfavored for many circumstances, mainly because of their large size (typically

* Corresponding authors at: College of Chemistry and Chemical Engineering, Henan University, Kaifeng, Henan 475004, PR China.
** Corresponding author.
E-mail addresses: hagren@kth.se (H. Ågren), chemwangl@henu.edu.cn (L. Wang), zhangjinglai@henu.edu.cn (J. Zhang), haichun@kth.se (H. Liu).

https://doi.org/10.1016/j.nanoen.2022.108015
Received 14 September 2022; Received in revised form 28 October 2022; Accepted 12 November 2022
Available online 15 November 2022

>20 nm), e.g., in subcellular imaging where sub-10 nm probes are preferable. In the imaging of subcellular structures, the smaller the size of the probes, the less interference they will cause on the objects and their functions, and the more readily they will be transported into and out of the organisms and cells [9]. There essentially exists a size (correspondingly a mass or volume) limitation, beyond which the use of luminescent probes is severely hampered. Although much effort has been devoted to developing small-scale UCNPs [17,18], it has been difficult to overcome the fact that they are strongly affected by surface quenching effects that usually make their luminescence very weak. Thus, surface passivation and sensitization effects need to be introduced in order to enhance the luminescence. However, currently developed strategies, based on e.g. the plasmon resonance effect [19], or use of inert shells [20], are usually accompanied with significantly increased particle mass (or volume, associated with the size), contrary to the original intention. As an illustration, Fig. 1a presents how the volume of a nanoparticle with different diameters increases after the growth of a shell with different thicknesses. For example, the volume of a nanoparticle with a diameter of 5 nm will increase by 2.7 after coating with a shell of merely 1 nm in thickness. This dramatic increase in the nanoparticle volume/mass with increasing the thickness of the shielding layer for ultrasmall UCNPs has not received sufficient attention.

One possible strategy, with limited effects on the particle size, is to use high concentration doping to maximize the proportion of optically active ions. However, this approach tends to lead to more severe surface quenching, because a high concentration of doping causes the excited energy to migrate efficiently in the active ion sub-lattice until it reaches the nanoparticle surface and dissipates (Fig. 1b) [21]. This effect is especially evident when the concentration of sensitizer ions (excitation light absorbers) is high. Therefore, there is an urgent need to develop more effective sensitization/passivation strategies to improve the luminescence performance of small-size UCNPs without exceeding the size/volume limitations.

In this work, we explore a transient energy trapping effect, previously identified in Er^{3+}-sensitized UCNPs [22,23], and prove that this effect can also function in the more popular and more efficient Yb^{3+}-sensitized UCNPs to confine the excitation energy inside the nanoparticles to boost upconversion luminescence. We further demonstrate that this energy trapping effect can be the basis for a surface passivation strategy that can produce superior sub-10 nm UCNPs, with much enhanced upconversion luminescence (by ~10 times) and with better resistance to environmental quenching but without increasing the size of the nanoparticles. The resultant bright ultrasmall UCNPs enable high-quality cell imaging as demonstrated here.

2. Results and discussion

2.1. Transient energy-trapping effect in Yb^{3+}-sensitized UCNPs

Recently, a transient energy trapping effect was identified in Er^{3+}-sensitized UCNPs [22], where Tm^{3+} ions were found able to confine the excitation energy inside the nanocrystals to combat energy-migration-induced luminescence surface quenching. Specifically, an optimal doping of Tm^{3+} into the Er^{3+}-based host leads to a trapping of the excitation energy at the $^3H_5$ state of Tm^{3+}, followed by a back-energy transfer process from the $^3H_5$ state of Tm^{3+} to the $^4I_{13/2}$ state of Er^{3+} [22], as depicted in Fig. 2a. The whole process effectively disrupts the lossy energy migration in the Er^{3+}-sublattice, preserves the excitation energy inside the nanocrystals, and serves as a positive energy feedback for populating the $^4F_{9/2}$ emitting state [22]. It was subsequently reported that other lanthanide ions, such as Ho^{3+} and Eu^{3+}, may also act as energy trapping centers in Er^{3+}-sensitized UCNPs to mitigate energy-migration-induced quenching [23]. We realize that this energy-level-mismatch-based effect may also function in Yb^{3+}-sensitized UCNPs. Yb^{3+}-sensitized UCNPs are among the ones with highest upconversion quantum yield and are most extensively used in various applications, benefitting from the large absorption cross-section of Yb^{3+} ions and high energy-transfer efficiency to other lanthanide emitters. However, they also suffer from severe energy-migration-drained surface quenching.

Previous studies may provide some clues for the inhibition on energy migration between Yb^{3+} ions by trapping centers. For the Yb-Er homogeneously doped UCNPs one finds in existing literature that the optimal doping concentration of Yb^{3+} ions is generally about 18–20 % [21,24]. However, in the Yb-Tm system, the optimal doping concentration of Yb^{3+} ions can be much higher, even above 60 % [25]. The results of our repeated experiments are also consistent with these previous reports (Figs. S1–S8). These results clearly show that higher Yb^{3+} doping concentrations in the Yb-Tm system do not infer the rapid energy dissipation caused by energy migration as that found in the Yb-Er system. Our in-depth mechanistic investigations disclose that the energy migration in the Yb^{3+} sub-lattice can be effectively disrupted by the Tm^{3+} ions, which inhibit the excitation-energy dissipation to the surface quenching sites and thus enhance the upconversion emission (see details in Section

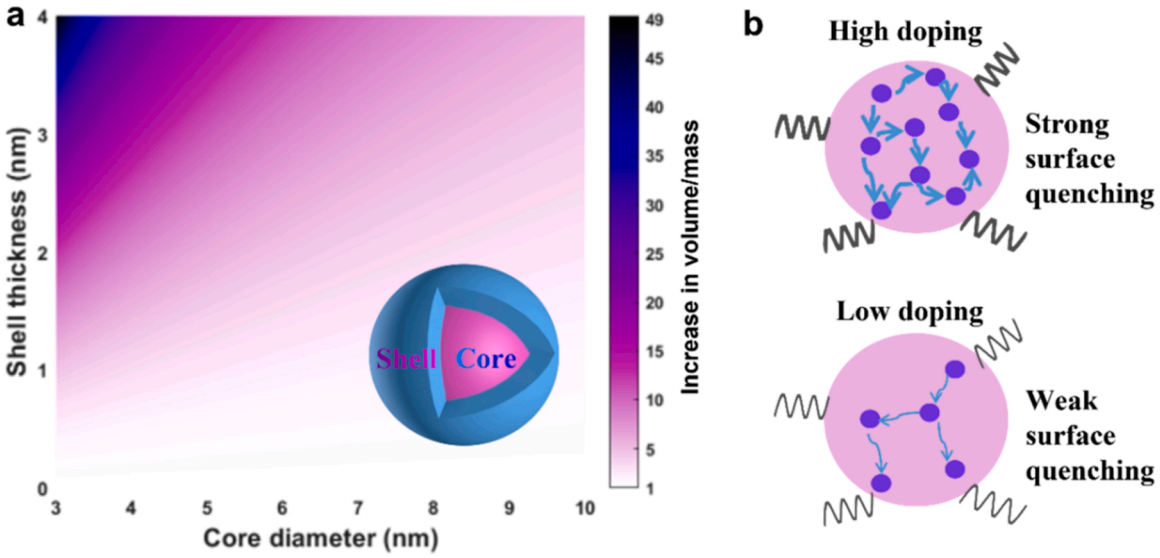

Fig. 1. **(a)** Estimation of the increase in the volume/mass of core-shell nanoparticles depending on the size of the initial core and the thickness of the added shell. **(b)** High-doping strategy leads to efficient energy migration and thereby strong surface quenching.

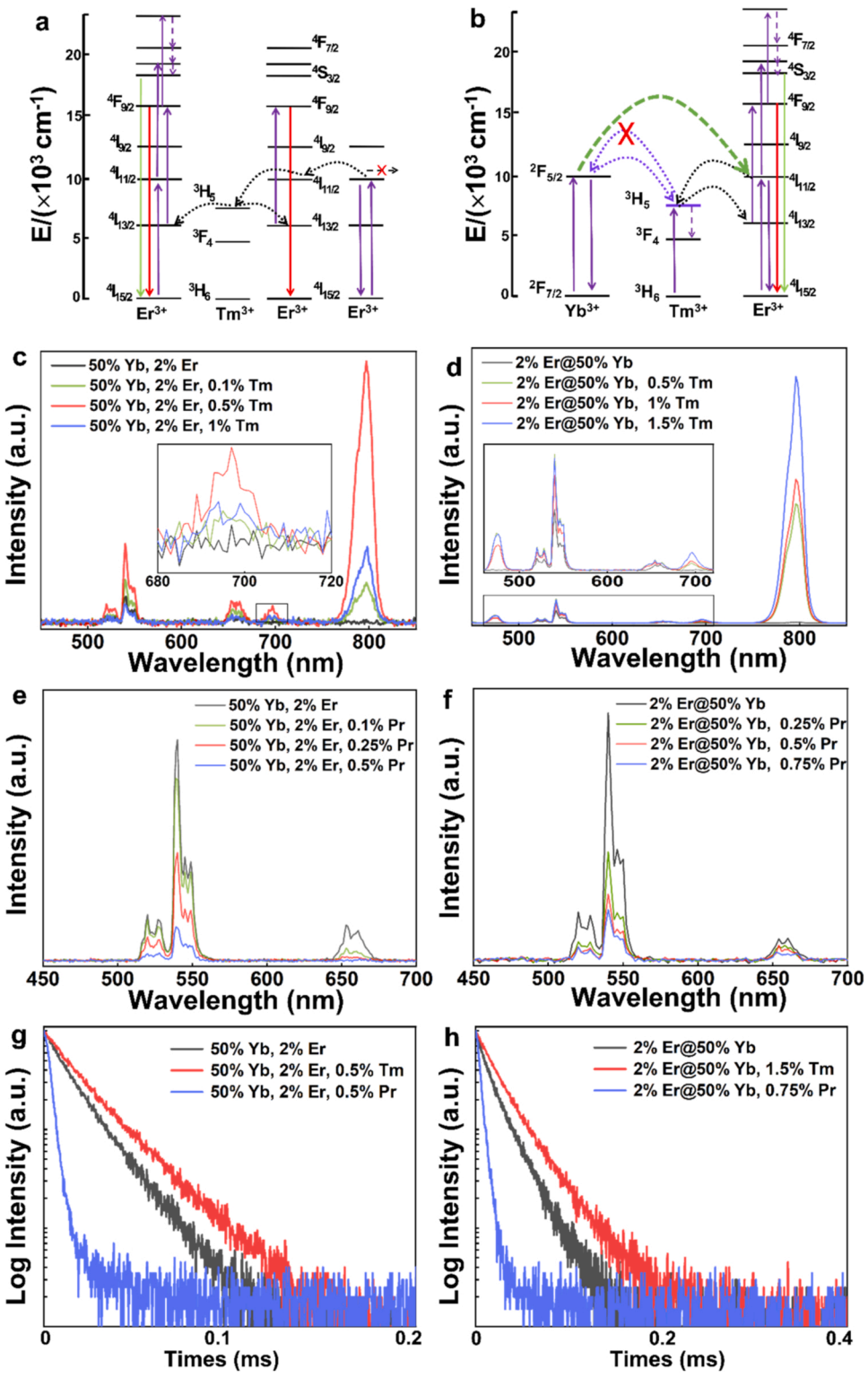

Fig. 2. (a) Transient energy trapping effect of Tm^{3+} in Er^{3+}-based host nanocrystals under excitation with a 980 nm diode laser. (b) Transient energy trapping effect of Tm^{3+} in Yb^{3+}-sensitized upconversion nanoparticles under excitation with a 980 nm diode laser. (c) Upconversion emission spectra of $NaYF_4$: 50 % Yb, 2 % Er, x % Tm (x = 0.1, 0.5, and 1) nanoparticles excited at 980 nm (50 W cm^{-2}). (d) Upconversion emission spectra of $NaYF_4$: 2% Er@$NaLuF_4$: 50 % Yb, x % Tm (x = 0.5, 1, and 1.5) nanoparticles excited at 980 nm (50 W cm^{-2}). (e) Upconversion emission spectra of $NaYF_4$: 50 % Yb, 2 % Er, x % Pr (x = 0.1, 0.25, and 0.5) nanoparticles excited at 980 nm (50 W cm^{-2}). (f) Upconversion emission spectra of $NaYF_4$: 2 % Er@$NaLuF_4$: 50 % Yb, x % Pr (x = 0.25, 0.5, and 0.75) nanoparticles excited at 980 nm (50 W cm^{-2}). (g) Decay curves of the Yb^{3+} emission in $NaYF_4$: 50 % Yb, 2 % Er, $NaYF_4$: 50 % Yb, 2 % Er, 0.5 % Tm, and $NaYF_4$: 50 % Yb, 2 % Er, 0.5 % Pr nanoparticles under the short-pulse excitation of a 980 nm diode laser. (h) Decay curves of the Yb^{3+} emission in $NaYF_4$: 2 % Er@$NaLuF_4$: 50 % Yb, $NaYF_4$: 2 % Er@$NaLuF_4$: 50 % Yb, 1.5 % Tm, and $NaYF_4$: 2 % Er@$NaLuF_4$: 50 % Yb, 0.75 % Pr nanoparticles under short-pulse excitation of a 980 nm diode laser.

2 in the Supporting information (SI)).

Next, we validated the inhibition effect of Tm^{3+} ions on the Yb^{3+} energy migration in Yb-Er-Tm homogeneously doped nanoparticles and assessed its effectiveness. $NaYF_4$: 50 % Yb, 2 % Er UCNPs were chosen as a model basis due to the well identified Yb^{3+} energy migration-induced quenching in such nanoparticles (Fig. S5b). A series of $NaYF_4$: 50 % Yb, 2 % Er UCNPs doped with different concentrations (0.1 %, 0.5 %, 1 %) of Tm^{3+} ions were synthesized, and TEM images show that the addition of Tm^{3+} ions at the studied concentrations did not cause noticeable changes in the nanoparticle size (25 nm, Fig. S9). The measured upconversion emission intensities of these nanoparticles under continuous-wave 980 nm excitation proved that after the tri-doping of Tm^{3+} ions, the characteristic upconversion emission bands of Tm^{3+} ions at 450, 475, 698 and 797 nm showed up where the Tm^{3+} 797 nm emission for 0.5 % Tm^{3+} doping was even stronger than the green and red emission bands of Er^{3+} ions (Fig. 2c). Intriguingly, the ignition of Tm^{3+} upconversion emission was not at a price of decreased Er^{3+} upconversion emission intensity. Instead, at low Tm^{3+} doping

concentrations (0.1 %, 0.5 %), the green upconversion emissions of Er^{3+} ions in the range of 500–570 nm were even significantly enhanced, e.g., by 3.2 folds for 0.5 % Tm^{3+} doping (Fig. 2c). These results verify that an optimal doping of Tm^{3+} ions can indeed improve the overall excitation-energy utilization efficiency and generate significantly stronger upconversion luminescence including that of the original Er^{3+} and the introduced Tm^{3+} emitters. Time-resolved spectroscopic characterization of these nanoparticles reveals that after an optimal doping of Tm^{3+} (0.5 %) the decay time of the Yb^{3+} excited state becomes significantly longer than that of the reference sample (Fig. 2g).

One question may be brought up here, namely that the upconversion emission enhancement effect found may be partially ascribed to the earlier mentioned energy trapping effect of Tm^{3+} ions on Er^{3+} energy migration (Fig. 2a) [22]. We speculated that this effect may not be the dominant effect considering the much lower doping concentration of Er^{3+} ions (2 %) in our case than in previous studies [22]. In order to investigate this, we synthesized core-shell structured $NaYF_4$: 2 % Er@$NaLuF_4$: 50 % Yb, x % Tm (x = 0, 0.5, 1, 1.5) nanoparticles. By separating Er^{3+} and Tm^{3+} in different layers, the influence of the Er^{3+}-Tm^{3+} direct interaction can be largely eliminated. We found that the Er^{3+} upconversion emission of Tm^{3+}-tridoped nanoparticles was still enhanced, together with the launching of strong Tm^{3+} upconversion emission (Fig. 2d). Considering the nanoparticle as a whole, after the Tm^{3+} tridoping, the integrated upconversion emission intensity from both the original Er^{3+} ions and the additional Tm^{3+} ions (400–850 nm) was greatly increased by a factor of 10.1. We also performed time-resolved spectroscopic studies on these nanoparticles and found that after an optimal doping of Tm^{3+} (1.5 %) the decay time of the Yb^{3+} excited state becomes significantly longer than that of the pristine $NaYF_4$: 2 % Er@$NaLuF_4$: 50 % Yb nanoparticles (Fig. 2h). These results confirm that Tm^{3+} doping can disrupt the energy migration in the Yb^{3+} sub-lattice and preserve more excitation energy inside the nanocrystals and so benefit the upconversion luminescence.

However, it is also notable that the optimal doping concentration of Tm^{3+} in $NaYF_4$: 50 % Yb, 2 % Er, x % Tm nanoparticle is 0.5 % (Fig. 2c), while that in $NaYF_4$: 2 % Er@$NaLuF_4$: 50 % Yb, x % Tm nanoparticle is 1.5 % (Fig. 2d). The significantly lower Tm^{3+} optimal doping concentration in Yb^{3+}-Er^{3+}-Tm^{3+} homogeneously doped UCNPs indeed reflects the direct interactions between Er^{3+} and Tm^{3+} in these nanocrystals. On the one hand, some direct-interaction route can contribute positively to the upconversion luminescence of Er^{3+} (Fig. 2b); and on the other hand, other interaction routes can compromise the gain of Er^{3+} upconversion luminescence, especially at elevated Tm^{3+} concentrations.

As control experiments, we selected another tri-dopant to tailor the nanoparticles, i.e., Pr^{3+}, which has a highly resonant energy state with the Yb^{3+} excited state (Fig. S10). As proved in our very recent study [8], the high resonance between the Pr^{3+} $^1G_4$ state and the Yb^{3+} $^2F_{5/2}$ state and their mutual interaction can even lead to high-efficiency photon avalanche effects. The addition of Pr^{3+} ions at the studied concentrations did not change the nanoparticle size either (Fig. S9). However, in contrast to the case of Tm^{3+} doping, the upconversion emission of Er^{3+} ions was severely quenched (Fig. 2e) without sufficient compensation from the Pr^{3+} emission. These results show that Pr^{3+} doping does not have the same function as Tm^{3+} to boost the upconversion emission in the Yb-Er nanoparticles. Some control experiments were also carried out in Er@Yb core-shell nanoparticles with Pr^{3+} ions as the additional dopants confined in the Yb^{3+}-containing shell layer, and similar Er^{3+} upconversion emission quenching was then observed (Fig. 2f). Here, the spatial separation of Pr^{3+} and Er^{3+} ions can exclude the influence of cross-relaxation between these two types of ions on the observed quenching of the Er^{3+} upconversion emission. These results point at that Pr^{3+} doping makes the energy migration in the Yb^{3+}-Er^{3+} system more deleterious to upconversion emission due to that its energy state ($^1G_4$) is resonant with the Yb^{3+} excited state.

Taken together, these experimental results prove the energy trapping effect of Tm^{3+} ions on disrupting the Yb^{3+} energy migration to preserve excitation energy inside the nanocrystals. In Yb^{3+}-Er^{3+}-Tm^{3+} homogeneously doped UCNPs, this transient energy trapping effect of Tm^{3+} ions is followed by a back-energy-transfer process from the $^3H_5$ state of Tm^{3+} to the $^4I_{13/2}$ state of Er^{3+} to further contribute to the upconversion luminescence of the latter (Fig. 2b). Crucially, applications of this effect will enable much more efficient use of the excitation energy absorbed by Yb^{3+} sensitizer ions without increasing the size of the nanoparticles.

2.2. Upconversion luminescence enhancement of small size UCNPs

This work was motivated by the possibility to produce bright ultrasmall UCNPs that can suffer less from surface quenching effect accelerated by energy-migration. We realized that the identified energy trapping effect can be employed as a surface passivation strategy for small UCNPs, which can potentially greatly enhance their upconversion luminescence but conserving the small size. As a next step we therefore tested this strategy on UCNPs of smaller size. For this purpose, we synthesized UCNPs with an average diameter of 5 nm. Here, $NaGdF_4$ was used as the matrix for such small size UCNPs due to the easier size control in this range for $NaGdF_4$-based nanoparticles compared to $NaYF_4$-based ones (referring to Section 1 in the SI for synthesis details). $NaGdF_4$: 30 % Yb, 2 % Er nanoparticles being Tm^{3+}-surface-modified are denoted as the "Doping group", while those without surface modification as the "Blank group". TEM characterization shows that these two groups of nanoparticles have the same size and regular morphology, being spherical in shape with an average diameter of about 5 nm, (Fig. 3a, b). Upconversion emission characterization shows that compared to the "Blank group", the Er^{3+} green (500–570 nm) and red (630–680 nm) upconversion emission intensities of the "Doping group" were increased by 9.7 and 6.2 times, respectively, together with strong Tm^{3+} emission at around 797 nm (Fig. 3c). We further compared the brightness of these two groups of nanoparticles on a single particle level using our previously established experimental protocol (subsection 1.6 in the SI). As shown in Fig. 3f–i, the "Doping group" nanoparticles showed much stronger green and red luminescence under the same excitation conditions using a 980 nm laser. The decay of the Yb^{3+} emission under short-pulse 980 nm excitation was also measured (Fig. 3d). It was found that the "Doping group" nanoparticles exhibited an obviously slower decay than the "Blank group", supporting our claim of the energy-migration-inhibition effect of the Tm^{3+} ions.

Turning to the optimization of small size nanoparticles and their use in biological environments, it becomes imperative to consider the quenching effect of water molecules. We expected that the inclusion of energy trapping ions would ameliorate the water quenching issue. In order to examine this contention, the oleic acid (OA) capping of UCNPs was initially removed using an acid-wash method with some modifications adopted from a previously reported protocol (see Section 1.5 in the SI for details), after which the UCNPs were redispersed in D_2O or D_2O/H_2O mixtures with varying content of H_2O. Fig. 3e presents the changes in intensities of different emission bands with increased water volume ratio. As can be seen in general, the upconversion emission intensities of both groups of nanoparticles decrease with increasing the proportion of H_2O. However, the upconversion emission of the "Doping group" is significantly better preserved than the "Blank group" with increasing presence of H_2O molecules. In addition, it is also notable that at a lower H_2O volume ratio, the increase in the water-quenching resistance of the "Doping group" is higher than at higher H_2O volume ratios. This indicates that the amount of incorporated Tm^{3+} ions using our protocol is not sufficient to completely suppress the quenching mechanism, particularly in an environment with a large proportion of H_2O. In the meantime, it also indicates that there might be room for further promotion of the water-quenching resistance if more Tm^{3+} ions can be introduced. In order to explore this possibility, we synthesized ultrasmall nanoparticles doped with higher Tm^{3+} concentration (3 %), denoted as the "High doping group", with the same protocol and performed water-quenching experiments. The results proved our

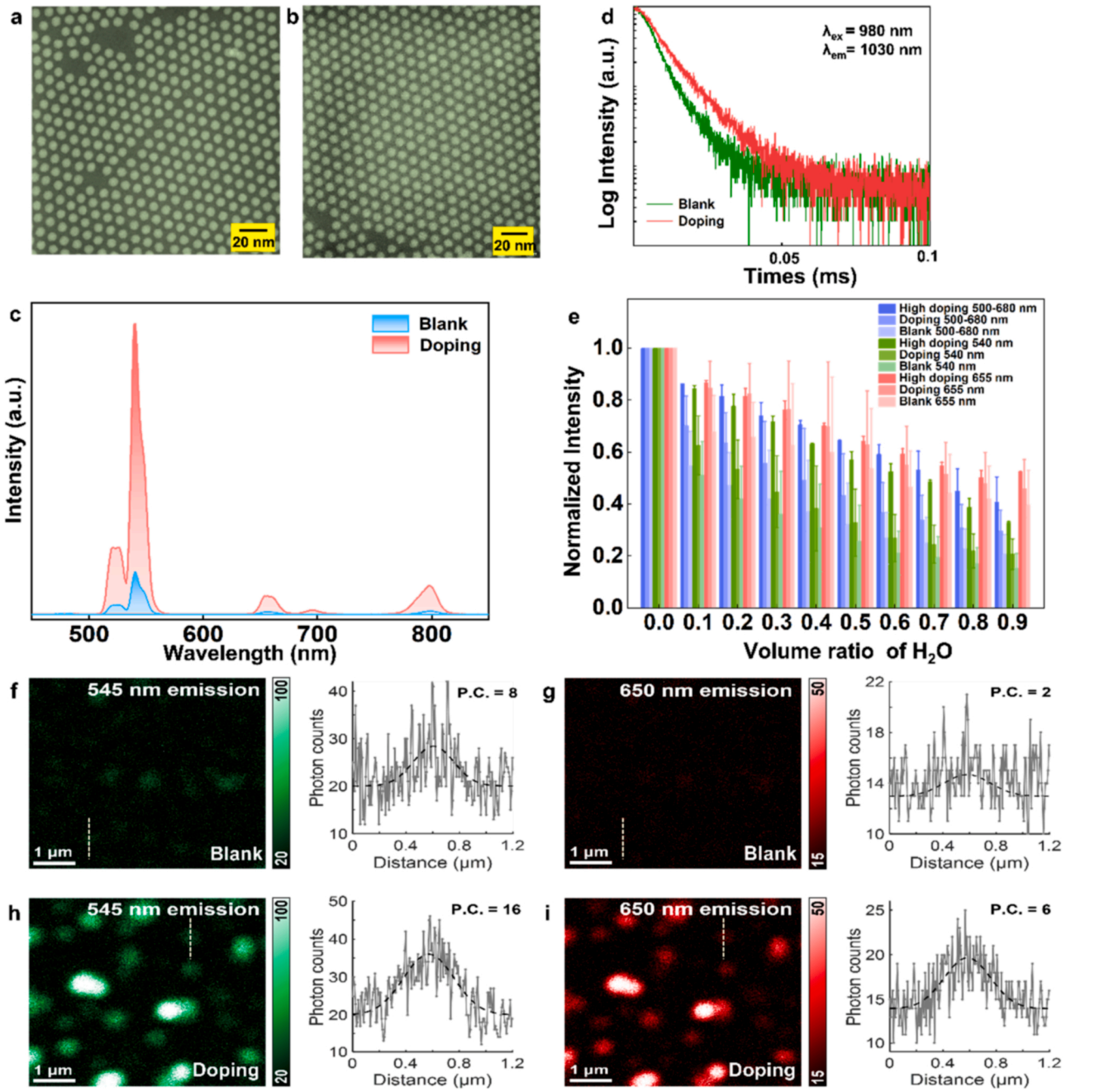

Fig. 3. (a) TEM image of $NaGdF_4$: 30 % Yb, 2 % Er nanoparticles (scale bar: 20 nm). (b) TEM image of $NaGdF_4$: 30 % Yb, 2 % Er nanoparticles with Tm^{3+} doped (scale bar: 20 nm). (c) Change in upconversion emission (under 980 nm excitation of 70 W cm^{-2}) of 5 nm $NaGdF_4$: 30 % Yb, 2 % Er nanoparticles after doping with Tm^{3+}. (d) Decays of the Yb^{3+} emission under short-pulse 980 nm excitation. (e) Quenching effect of the increasing content of H_2O on the upconversion emission of nanoparticles undoped and doped with Tm^{3+} damping ions (Doping – 0.5 % Tm, High doping – 3 % Tm) under 980 nm excitation. (f) and (g) are multiphoton laser scanning microscopic quantitative measurements of the 545 nm and 650 nm emission of a single "Blank" nanoparticle, respectively. The power density of the excitation laser was kept at 100 kW cm^{-2}. Pixel dwelling times: 200 μs. (h) and (i) are multiphoton laser scanning microscopic quantitative measurements of the 545 nm and 650 nm emission of a single "Doping" nanoparticle, respectively. The power density of the excitation laser was kept at 100 kW cm^{-2}. Pixel dwelling times: 200 μs.

speculation that increasing the concentration of Tm^{3+} ions can further improve the water-quenching resistance (Fig. 3e). However, we also like to point out that the 3 % doping level of Tm^{3+} is not optimal in terms of upconversion luminescence intensity.

2.3. Labeling and imaging of cells using ultrasmall UCNPs

As a proof of the outstanding quality of our nanoparticles, we performed labeling and imaging of HeLa cells using ultrasmall UCNPs (both the "Blank" and the "Doping" groups), using our previous protocols (see the SI for details) [8]. UCNPs were surface modified by polyacrylic acid (PAA), the carboxyl group of PAA was activated, and then the nanoparticles were conjugated with Phalloidin. HeLa cells were cultured and labeled according to commonly used culture methods and immunostaining techniques [8]. These immunostained HeLa cells were imaged on a multiphoton laser-scanning microscope equipped with a 975-nm laser. As shown in Fig. 4, when the "Blank" nanoparticles were used to label the cells, the upconversion luminescence at 545 nm and 650 nm

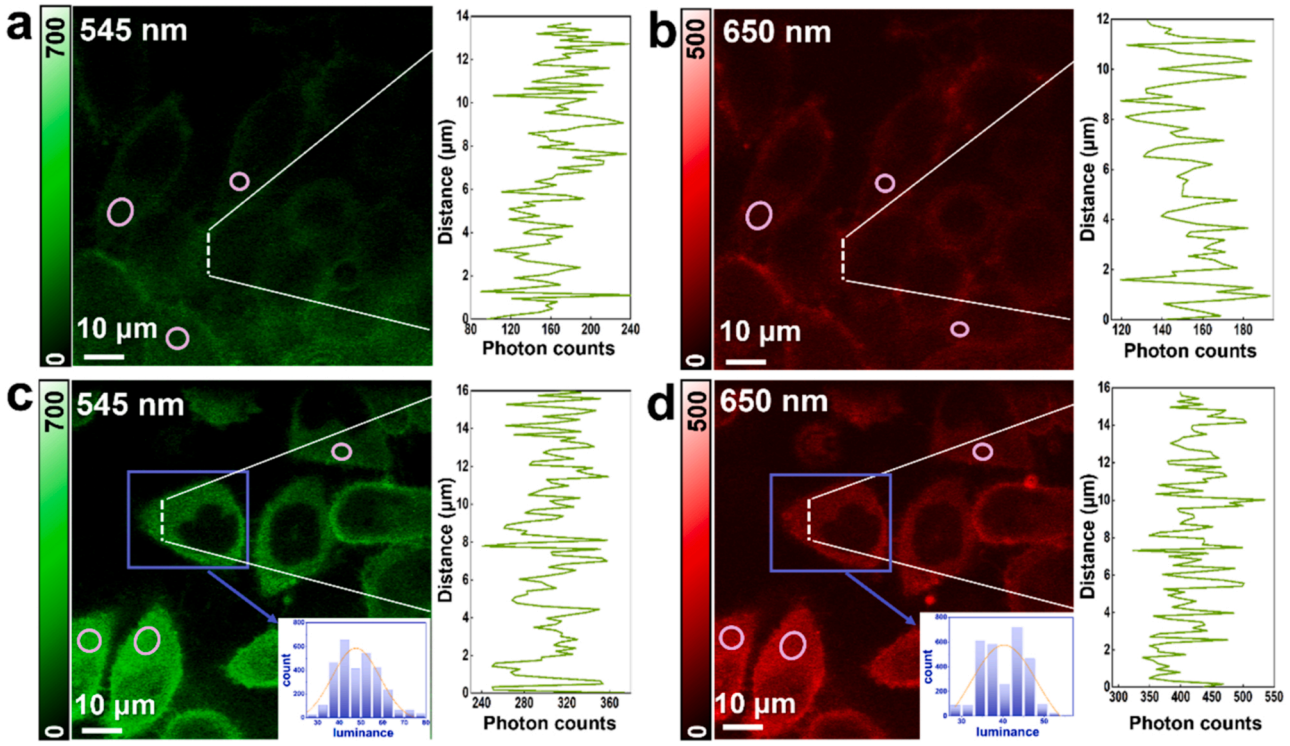

Fig. 4. (a), (b) Labeling and imaging of HeLa cells using the "Blank" UCNPs. (c), (d) Labeling and imaging of HeLa cells using the "Doping" UCNPs. The luminescence intensity line profiles next to the cell images were extracted from the regions marked by dashed lines. Circles in (a)–(d) mark the selected areas in quantifying the enhancement factors of upconversion luminescence intensities. The blue boxes in (c) and (d) represent the selected cell for evaluating the degree of intensity variation of the upconversion luminescence, which are shown in the lower right insets.

became rather dim (Fig. 4a–b). However, with the "Doping" nanoparticle labeling the cells emit much brighter upconversion luminescence under the same test conditions (Fig. 4c–d). In order to quantify the enhancement factors, we selected several areas in Fig. 4a and c, and in Fig. 4b and d (marked with circles), and calculated the ratios of the average photon counts. The enhancement factors for the green and red channels were roughly estimated to be 3.1 and 2.2, respectively. In addition, it is emphasized that our imaging results show very uniform spatial distribution of the ultrasmall UCNPs in the outer nuclear region, rendering a very clear cell nuclear boundary (Fig. 4c–d). The degree of variation of the luminescence intensity (the ratio between the intensity standard deviation and the average intensity) in the outer nuclear region in a selected cell (marked with squares in Fig. 4c–d) was further calculated, giving only 12.5 % for the 545 nm emission and 12.9 % for the 650 nm emission (intensity histograms are shown in the insets of Fig. 4c–d; Table S1).

In previous reports in the literatures, it has been common to use UCNPs for cell labeling and imaging, but with the UCNP size being mostly around 20 nm [26–38]. By observing and comparing the cell imaging results from these reports, we found that the UCNPs around 20 nm were usually not distributed evenly in the cells and that they apparently easily could accumulate, leading to a degradation of the imaging quality (Fig. S11) [26–38]. We calculated the degree of variation of the luminescence intensity of cell imaging using UCNPs in two selective Refs. [30,33], using the same surface modification and functionalization methods for the UCNPs as in our work. The calculated degrees of intensity variation (59.2 % in Ref. [30], 78.4 % in Ref. [33], Table S1) are much larger than that in our imaging results. In addition, due to the aggregation and uneven distribution of the nanoparticles, no clear cell nuclear boundaries comparable to ours can be discerned in the imaging results using ~ 20 nm UCNPs (Fig. S11) [26–38].

3. Conclusion

The present work was motivated by the fact that considerable difficulties are encountered in producing upconversion nanoparticles (UCNPs) that are sufficiently small to be effectively used as minimally interfering luminescent probes for biological applications. This is unfortunate, since the use of UCNPs otherwise would bring about a number of advantages for such applications. In order to improve the upconversion emission, researchers have tried a variety of methods, but that inevitably increased the size of the nanoparticles, which in turn leads to limited abilities to penetrate and reach intended targets, suffering from steric constraints and interference with the studied objects. We here explored a previously identified transient energy trapping effect, reported to be prominent in highly doped Er^{3+}-sensitized UCNPs [22,23] and extended it to the more popular and efficient Yb^{3+}-sensitized UCNPs. We proposed a concept to use the trapping effect to solve the size-brightness dilemma of UCNPs, namely to use energy trapping ions to suppress the energy migration between the optically active ions and thereby to block the surface quenching that deactivates the luminescence of the particles while maintaining a small nanoparticle size. We applied this strategy to sub-10 nm UCNPs and obtained significant luminescence enhancement and better resistance to water-induced quenching, in fact an unprecedented high-quality cell labeling and imaging could be achieved. Our work thus provides an approach to solve the problem of surface quenching affecting ~ 5 nm nanoparticles, which will pave the way for further applications of UCNPs. This, we believe, will have wide ramifications for sub-cellular imaging and also for other biomedical applications where the proper biodistribution of the UCNP labels is a major limitation.

CRediT authorship contribution statement

Fuhua Huang: Investigation, Data curation, Writing – original draft,

Visualization. **Lucía Labrador-Páez:** Investigation, Data curation, Formal anályis, Writing – original draft, Visualization. **Hans Ågren:** Resources, Writing – original draft, Supervision, Funding acquisition. **Li Wang:** Resources, Supervision, Funding acquisition. **Jinglai Zhang:** Resources, Supervision, Funding acquisition. **Rui Pu:** Investigation, Data curation, Formal analysis, Visualization. **Qiuqiang Zhan:** Investigation, Formal analysis. **Jerker Widengren:** Formal analysis, Writing – original draft, Funding acquisition. **Haichun Liu:** Conceptualization, Methodology, Validation, Formal analysis, Writing – original draft, Supervision, Project administration, Funding acquisition.

Declaration of Competing Interest

The authors declare that they have no known competing financial interests or personal relationships that could have appeared to influence the work reported in this paper.

Acknowledgements

We are grateful for the support of “Henan Engineering Research Center of Green Anticorrosion Technology for Magnesium Alloy”. This work was supported by the National Natural Science Foundation of China (22178086), Program of Henan Center for Outstanding Overseas Scientists (GZS2020011), Henan University’s First-Class Discipline Science and Technology Research Project (2018YLTD07), and the Excellent Foreign Experts Project of Henan University. H.L. acknowledges support from the Swedish Research Council (VR 2016-03804), the Carl Tryggers Foundation (CTS 18: 229, CTS 21: 1208), the ÅForsk Foundation (19-424), and the Olle Engkvists Foundation (200-0514). J.W. acknowledges support from the Swedish Foundation for Strategic Research (SSF ITM17-0491). Q.Z. acknowledges support from the National Natural Science Foundation of China (62122028, 11974123), the Guangdong Provincial Science Fund for Distinguished Young Scholars (2018B030306015). Helpful comments by Prof. Paras N. Prasad, University of Buffalo are appreciated.

Data Availability

All the relevant data that support the findings of this work are available from the correspondence authors upon reasonable request.

Appendix A. Supporting information

Supplementary data associated with this article can be found in the online version at doi:10.1016/j.nanoen.2022.108015.

References

[1] D. Asanuma, Y. Takaoka, S. Namiki, K. Takikawa, M. Kamiya, T. Nagano, Y. Urano, K. Hirose, Acidic-pH-activatable fluorescence probes for visualizing exocytosis dynamics, Angew. Chem. Int. Ed. 53 (2014) 6085–6089.
[2] D.S. Bindels, L. Haarbosch, L. Van Weeren, M. Postma, K.E. Wiese, M. Mastop, S. Aumonier, G. Gotthard, A. Royant, M.A. Hink, mScarlet: a bright monomeric red fluorescent protein for cellular imaging, Nat. Methods 14 (2017) 53–56.
[3] H. Liu, X. Deng, S. Tong, C. He, H. Cheng, Z. Zhuang, M. Gan, J. Li, W. Xie, P. Qiu, In vivo deep-brain structural and hemodynamic multiphoton microscopy enabled by quantum dots, Nano Lett. 19 (2019) 5260–5265.
[4] K. Gorshkov, K. Susumu, J. Chen, M. Xu, M. Pradhan, W. Zhu, X. Hu, J.C. Breger, M. Wolak, E. Oh, Quantum dot-conjugated SARS-CoV-2 spike pseudo-virions enable tracking of angiotensin converting enzyme 2 binding and endocytosis, ACS Nano 14 (2020) 12234–12247.
[5] Y. Li, Z. Cai, S. Liu, H. Zhang, S.T. Wong, J.W. Lam, R.T. Kwok, J. Qian, B.Z. Tang, U1 snRNP regulates cancer cell migration and invasion in vitro, Nat. Commun. 11 (2020) 1–10.
[6] C.T. Xu, P. Svenmarker, H. Liu, X. Wu, M.E. Messing, L.R. Wallenberg, S. Andersson-Engels, High-resolution fluorescence diffuse optical tomography developed with nonlinear upconverting nanoparticles, ACS Nano 6 (2012) 4788–4795.
[7] X. Guo, R. Pu, Z. Zhu, S. Qiao, Y. Liang, B. Huang, H. Liu, L. Labrador-Páez, U. Kostiv, P. Zhao, Author correction: visualizing group II intron dynamics between the first and second steps of splicing, Nat. Commun. 13 (2022) 1–10.
[8] Y. Liang, Z. Zhu, S. Qiao, X. Guo, R. Pu, H. Tang, H. Liu, H. Dong, T. Peng, L.-D. Sun, Migrating photon avalanche in different emitters at the nanoscale enables 46th-order optical nonlinearity, Nat. Nanotechnol. 17 (2022) 524–530.
[9] Q. Zhan, H. Liu, B. Wang, Q. Wu, R. Pu, C. Zhou, B. Huang, X. Peng, H. Ågren, S. He, In situ click chemistry generation of cyclooxygenase-2 inhibitors, Nat. Commun. 8 (2017) 1–11.
[10] A.M. Kotulska, A. Pilch-Wrobel, S. Lahtinen, T. Soukka, A. Bednarkiewicz, Upconversion FRET quantitation: the role of donor photoexcitation mode and compositional architecture on the decay and intensity based responses, Light Sci. Appl. 11 (2022) 256.
[11] A. Bansal, H. Liu, M.K.G. Jayakumar, S. Andersson-Engels, Y. Zhang, Quasi-continuous wave near-infrared excitation of upconversion nanoparticles for optogenetic manipulation of C. elegans, Small 12 (2016) 1732–1743.
[12] Y. Ma, J. Bao, Y. Zhang, Z. Li, X. Zhou, C. Wan, L. Huang, Y. Zhao, G. Han, T. Xue, Mammalian near-infrared image vision through injectable and self-powered retinal nanoantennae, Cell 177 (2019) 243–255 (.e215).
[13] Y. Pan, J. Yang, X. Luan, X. Liu, X. Li, J. Yang, T. Huang, L. Sun, Y. Wang, Y. Lin, Near-infrared upconversion-activated CRISPR-Cas9 system: A remote-controlled gene editing platform, Sci. Adv. 5 (2019) eaav7199.
[14] G. Chen, H. Qiu, P.N. Prasad, X. Chen, Upconversion nanoparticles: design, nanochemistry, and applications in theranostics, Chem. Rev. 114 (2014) 5161–5214.
[15] M. Xu, B. Xue, Y. Wang, D. Wang, D. Gao, S. Yang, Q. Zhao, C. Zhou, S. Ruan, Z. Yuan, Temperature-feedback nanoplatform for NIR-II penta-modal imaging-guided synergistic photothermal therapy and CAR-NK immunotherapy of lung cancer, Small 17 (2021), 2101397.
[16] Z. Gong, T. Wu, X. Chen, J. Guo, Y. Zhang, Y. Li, Upconversion nanoparticle decorated spider silks as single-cell thermometers, Nano Lett. 21 (2021) 1469–1476.
[17] H. Li, L. Xu, G. Chen, Controlled synthesis of monodisperse hexagonal NaYF4:Yb/Er nanocrystals with ultrasmall size and enhanced upconversion luminescence, Molecules 22 (2017) 2113.
[18] A.D. Ostrowski, E.M. Chan, D.J. Gargas, E.M. Katz, G. Han, P.J. Schuck, D. J. Milliron, B.E. Cohen, Controlled synthesis and single-particle imaging of bright, sub-10 nm lanthanide-doped upconverting nanocrystals, ACS Nano 6 (2012) 2686–2692.
[19] Y. Gao, S. Murai, K. Shinozaki, S. Ishii, K. Tanaka, Aluminum for near infrared plasmonics: amplified up-conversion photoluminescence from core–shell nanoparticles on periodic lattices, Adv. Opt. Mater. 9 (2021), 2001040.
[20] A. Lay, C. Siefe, S. Fischer, R.D. Mehlenbacher, F. Ke, W.L. Mao, A.P. Alivisatos, M. B. Goodman, J.A. Dionne, Bright, mechanosensitive upconversion with cubic-phase heteroepitaxial core-shell nanoparticles, Nano Lett. 18 (2018) 4454–4459.
[21] L. Sun, R. Gao, T. Pan, X.-C. Ai, L. Fu, J.-P. Zhang, Concentration-regulated photon upconversion and quenching in $NaYF_4$:Yb^{3+},Er^{3+} nanocrystals: nonexponentiality revisited, Nanoscale 11 (2019) 18150–18158.
[22] Q. Chen, X. Xie, B. Huang, L. Liang, S. Han, Z. Yi, Y. Wang, Y. Li, D. Fan, L. Huang, X. Liu, Confining excitation energy in Er^{3+}-sensitized upconversion nanocrystals through Tm^{3+}-mediated transient energy trapping, Angew. Chem. 129 (2017) 7713–7717.
[23] Y. Shang, S. Hao, W. Lv, T. Chen, L. Tian, Z. Lei, C. Yang, Confining excitation energy of Er^{3+}-sensitized upconversion nanoparticles through introducing various energy trapping centers, J. Mater. Chem. C 6 (2018) 3869–3875.
[24] M. Wang, Y. Tian, F. Zhao, R. Li, W. You, Z. Fang, X. Chen, W. Huang, Q. Ju, Alleviating the emitter concentration effect on upconversion nanoparticles via an inert shell, J. Mater. Chem. C 5 (2017) 1537–1543.
[25] X. Zheng, S. Shikha, Y. Zhang, Elimination of concentration dependent luminescence quenching in surface protected upconversion nanoparticles, Nanoscale 10 (2018) 16447–16454.
[26] C. Wang, L. Cheng, Z. Liu, Drug delivery with upconversion nanoparticles for multi-functional targeted cancer cell imaging and therapy, Biomaterials 32 (2011) 1110–1120.
[27] W. Zhang, B. Peng, F. Tian, W. Qin, X. Qian, Facile preparation of well-defined hydrophilic core-shell upconversion nanoparticles for selective cell membrane glycan labeling and cancer cell imaging, Anal. Chem. 86 (2014) 482–489.
[28] Z. Zhang, M.K.G. Jayakumar, S. Shikha, Y. Zhang, X. Zheng, Y. Zhang, Modularly assembled upconversion nanoparticles for orthogonally controlled cell imaging and drug delivery, ACS Appl. Mater. 12 (2020) 12549–12556.
[29] L. Zhang, C. Chen, S.S. Tay, S. Wen, C. Cao, M. Biro, D. Jin, M.H. Stenzel, Optimizing the polymer cloak for upconverting nanoparticles: an evaluation of bioactivity and optical performance, ACS Appl. Mater. 13 (2021) 16142–16154.
[30] Q. Chen, C. Wang, L. Cheng, W. He, Z. Cheng, Z. Liu, Protein modified upconversion nanoparticles for imaging-guided combined photothermal and photodynamic therapy, Biomaterials 35 (2014) 2915–2923.
[31] S. Zeng, Z. Yi, W. Lu, C. Qian, H. Wang, L. Rao, T. Zeng, H. Liu, H. Liu, B. Fei, Simultaneous realization of phase/size manipulation, upconversion luminescence enhancement, and blood vessel imaging in multifunctional nanoprobes through transition metal Mn^{2+} doping, Adv. Funct. Mater. 24 (2014) 4051–4059.
[32] X. Zou, M. Xu, W. Yuan, Q. Wang, Y. Shi, W. Feng, F. Li, A water-dispersible dye-sensitized upconversion nanocomposite modified with phosphatidylcholine for lymphatic imaging, Chem. Commun. 52 (2016) 13389–13392.
[33] P. Wang, F. Zhou, K. Guan, Y. Wang, X. Fu, Y. Yang, X. Yin, G. Song, X.-B. Zhang, W. Tan, In vivo therapeutic response monitoring by a self-reporting upconverting covalent organic framework nanoplatform, Chem. Sci. 11 (2020) 1299–1306.
[34] M. Wang, C.-C. Mi, W.-X. Wang, C.-H. Liu, Y.-F. Wu, Z.-R. Xu, C.-B. Mao, S.-K. Xu, Immunolabeling and NIR-excited fluorescent imaging of HeLa cells by using NaYF(4):Yb,Er upconversion nanoparticles, ACS Nano 3 (2009) 1580–1586.

[35] Q. Liu, W. Feng, T. Yang, T. Yi, F. Li, Upconversion luminescence imaging of cells and small animals, Nat. Protoc. 8 (2013) 2033–2044.
[36] H. Du, L. Zhang, W. Mao, Y. Zhao, H. Huang, Y. Xiao, Y. Zhang, X. He, K. Wang, Ultrafine fluorene-pyridine oligoelectrolyte nanoparticles for supersensitive fluorescence sensing of heparin and protamine, Chem. Commun. 57 (2021) 8304–8307.
[37] J. Liu, N. Li, R. Wu, Y. Zhao, Q. Zhan, S. He, Sub-5-nm lanthanide-doped ZrO_2@NaYF_4 nanodots as efficient upconverting probes for rapid scanning microscopy and aptamer-mediated bioimaging, Opt. Mater. Express 5 (2015) 1759–1771.
[38] L.-L. Li, P. Wu, K. Hwang, Y. Lu, An exceptionally simple strategy for DNA-functionalized up-conversion nanoparticles as biocompatible agents for nanoassembly, DNA delivery, and imaging, J. Am. Chem. Soc. 135 (2013) 2411–2414.

Fuhua Huang, a PhD candidate at the School of Chemistry and Chemical Engineering, Henan University (China). Her research interests focus on the optical properties of upconversion nanomaterials.

Lucía Labrador-Páez got her PhD degree from the Autonomous University of Madrid. Then she was postdoctoral researcher at the Experimental Biomolecular Physics Group at KTH Royal Institute of Technology, Sweden. Currently, she is Assistant Professor at the Complutense University of Madrid (Spain). Her research explores the interaction of water and luminescent materials.

Hans Ågren, graduated 1979 as PhD at Uppsala University, Sweden. He became the first holder of the chairs in Computational Physics at Linköping University in 1990 and in Theoretical Chemistry at the Royal Institute of Technology, Stockholm in 1998. His research activities concern molecular/nano/bio photonics and electronics, computational nano- and bio-technology, being a mix of method development and problem oriented applications. He participates in a number of international networks and hold several guest professorships. Among awarded prices, one can mention the Swedish Bjurzon award, the Björn Roos award and the Changjiang Distinguished Professorship awarded by the Ministry of Education of China.

Li Wang, received her Ph.D degree from the Jilin University (China). She then was a senior fellow in the Department of Chemistry, National University of Singapore. Curently, she is the distinguished professor and doctoral supervisor of Henan University (China). Her research interests include synthesis and application of nano-transformed materials on rare earth and design and development of multi-functional coatings with nano-materials on magnesium alloys.

Jinglai Zhang, received his Ph.D degree from the Sichuan University (China). Currently, he is the distinguished professor and doctoral supervisor of Henan University (China). His research interests include the design and development of catalysts for carbon dioxide conversion and synthesis and application of nano-transformed materials on rare earth.

Rui Pu received his Bachelor degree in Optical Information Science and Technology at South China Normal University, China. Since then he has been studying as a PhD student in Optics at South China Normal University, China. His research interests include super-resolution fluorescence microscopy and photon upconversion.

Qiuqiang Zhan is currently a professor in South China Normal University, China. He received his Bachelor degree in Optics from Shandong University, and his Ph.D degree in Optical Engineering at Zhejiang University. He had visiting research in Lund University, Sweden and the Chinese University of Hong Kong. His research interests include fluorescence microscopy and photon upconversion. As the first/corresponding author, he has published 40 peer-reviewed journal (including Nature Nanotechnology, Nature Communications) papers. He has won some awards for his creative works, including "National Excellent Young Scholars" "Distinguished Young Scholars of Guangdong", "Hong Kong Scholar award" and "Youth Innovation Award".

Jerker Widengren is professor in Experimental Biomolecular Physics at KTH Royal Institute of Technology and belongs to the pioneers of fluorescence-based single-molecule detection (SMD) and fluorescence correlation spectroscopy (FCS). The focus of his research group is on development of fluorescence-based ultrasensitive and ultrahigh resolution spectroscopy/microscopy techniques, their application for biomolecular and cellular studies and towards diagnostic applications. The group was among the very first to start with stimulated emission depletion (STED) super-resolution microscopy (SRM) and its use for sub-cellular characterization and diagnostics. It has also developed transient state (TRAST) spectroscopy/microscopy to follow photodynamics of emitting species, which is a particular focus of the group.

Haichun Liu received his Bachelor degree in optical information science and technology and his M.Sc. degree in optics at Harbin Institute of Technology, China, and his PhD degree in physics at Lund University, Sweden. He is currently a researcher at KTH Royal Institute of Technology, Sweden. His research interests include healthcare and energy applications of photonic nanomaterials, and super-resolution fluorescence microscopy.